

# SMD Compatible Ku-band LTCC Circulators

Norbert Parker<sup>(1)</sup>, Camilla Kärfelt<sup>(1)</sup>, Richard Lebourgeois<sup>(2)</sup>, Vincent Laur<sup>(3)</sup>, Laurent Roussel<sup>(4)</sup>

<sup>(1)</sup>Lab-STICC UMR CNRS 6285, IMT-Atlantique  
Campus de Brest, Technopôle Brest-Iroise,  
CS 83818, 29238 Brest cedex 03, France  
Email: {norbert.parker, camilla.karfelt}@imt-atlantique.fr

<sup>(2)</sup>Thales Research & Technology  
Campus Polytechnique  
1 Avenue Augustin Fresnel  
F-91767 Palaiseau Cedex France

<sup>(3)</sup>Lab-STICC UMR CNRS 6285, Université de Bretagne Occidentale  
6, Avenue le Gorgeu,  
CS 93837, F-29238 Brest Cedex 3, France  
Email: vincent.laur@univ-brest.fr

<sup>(4)</sup>Thales Land & Air Systems  
2 Avenue Gay Lussac  
F-78990 Élancourt, France

## INTRODUCTION

The use of Y-junction circulators is hindered by their high cost, large size and complicated integration into a system. To address the issue of price, the potential of using the low-temperature co-fired ceramic (LTCC) technology has been studied in the literature [1]-[5]. The benefit of this manufacturing technology is that it streamlines the intricate production process of these components (ceramic machining, gluing...) while simultaneously yielding a monolithic substrate, thus decreasing fabrication cost.

It was demonstrated that good performance with low losses can be achieved using the LTCC technology in Ku-band [6]. The current investigation aims to use this technology to mitigate the other two main downsides mentioned previously, compactness and ease of integration. Indeed, the 2.5D nature of the technology allows the integration of solder pads and vias compatible with the surface-mounted component (SMD) technology into the substrate.

The structure of the circulator and the PCB is shown in Fig. 1. The metallization topology of the circulator is a Y-junction in microstrip topology. The metallization of the circulator is made of silver. A single permanent magnet placed on a dielectric spacer polarizes the ferrite.

In this paper, the design of SMD circulators compatible with a LTCC process will be at first described. Then, the fabrication steps and measurement of two circulators based on garnet or spinel ferrites will be detailed.

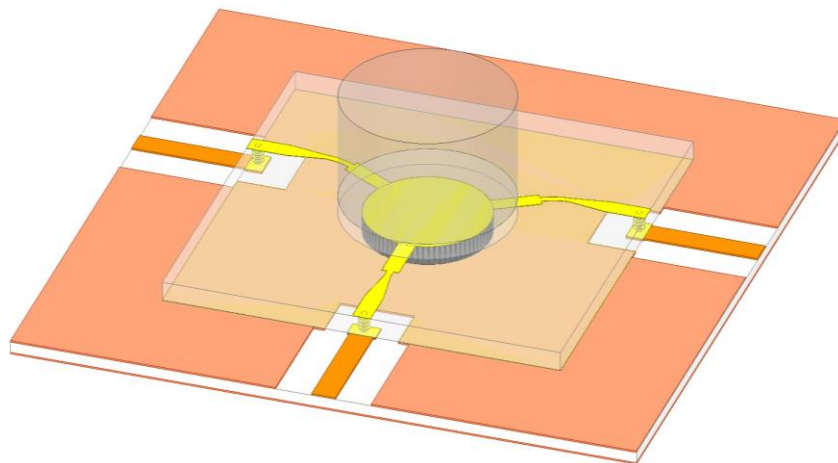


Fig. 1. SMD Circulator and the PCB

## SMD CIRCULATOR DESIGN

### Material properties and simulation configuration

The dielectric and magnetic properties of the selected materials are given in **Erreur ! Source du renvoi introuvable.**. These material properties are used to design two Ku-band circulators. The permanent magnet used to polarize the ferrite is a Samarium-Cobalt Magsy magnet, reference YXG-28. Its diameter is 3mm and its height is 2mm. Due to the high conductivity of the magnet, it is placed on a 300 $\mu$ m Teflon spacer above the circulator in order to avoid the resonator to be short-circuited. The substrate of the circulator consists of a high permittivity dielectric, which houses the SMD connectors and access lines, and a ferrite disc positioned under the central circular resonator. The ferrites used are a garnet ferrite and a spinel ferrite whose sintering temperature is below 950°C. They have been specifically developed to be compatible with the LTCC technology and to be used in circulators. They have previously been used in [6]. The garnet ferrite exhibits moderate saturation magnetization but high permittivity, while the spinel ferrite exhibits high magnetization and moderate permittivity.

The simulation software used is the Ansys HFSS electromagnetic solver. The internal magnetic field inside the ferrite, generated by the permanent magnet, is determined by the Ansys Maxwell3D magnetostatic solver. Doing so allows the non-uniformity of the static field inside the ferrite to be accounted for.

The SMD transitions and Y-junction are designed separately and then combined to simulate the SMD component.

Table 1. Material properties

Material	$\epsilon_r$	$\tan\delta$	$4\pi M_s$ (G)	$\Delta H$ (Oe)
Garnet	21	$3.10^{-3}$	1900	100
Spinel	13	$1.10^{-3}$	3800	100
VLF220Aq4	21	$1.10^{-3}$	-	-
Teflon <sup>TM</sup>	2.1	$1.10^{-3}$	-	-

### Design of the SMD transition

The connection between the two sides of the component required to make an SMD junction is usually made using a via located at the edge of the substrate, so that when the final component is trimmed, a metallized half-via is located at the edge. This configuration is illustrated in Fig. 2. However, this topology is not compatible with the LTCC manufacturing technology. Therefore, this transition must be modified to comply with the fabrication process, especially regarding the via used.

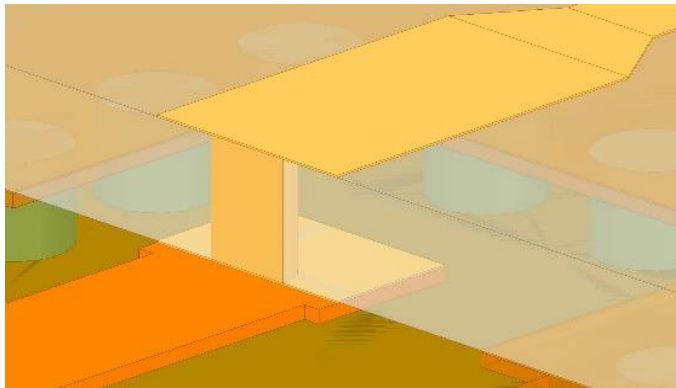


Fig. 2. SMD transition using a metallized half-via

The thickness of the reported component is 352 $\mu$ m. This value corresponds to a stack of four material layers. The two faces are connected by a 100 $\mu$ m via. The manufacturing technology requires each layer to be metallized independently prior to assembly. The vias on each layer are metallized using a circular 200 $\mu$ m diameter metallization pattern. As a result, the transition topology consists of a via with metallized circles at the interface between each layer (Fig. 3). The PCB substrate is a 203 $\mu$ m sheet of Rogers 4003.

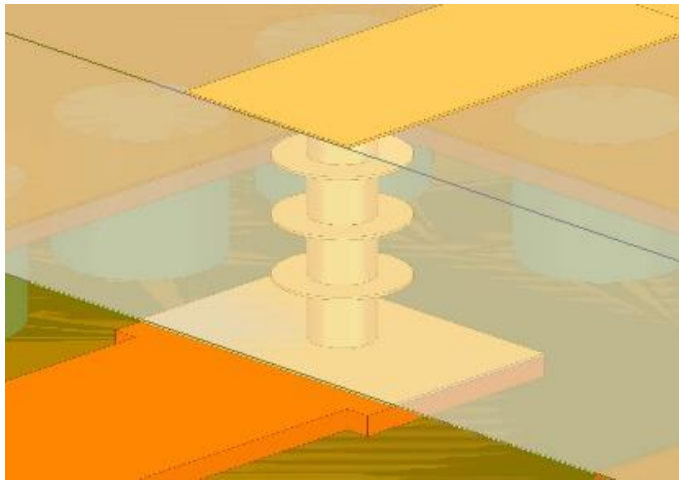


Fig. 3. SMD transition using a metallized half-via

The transition performance is evaluated with the simulation of a soldered microstrip line. The simulated S parameters are shown in Fig. 4. A return loss higher than 20dB over the frequency band of interest (~15-21GHz) is achieved through the optimization of the transition.

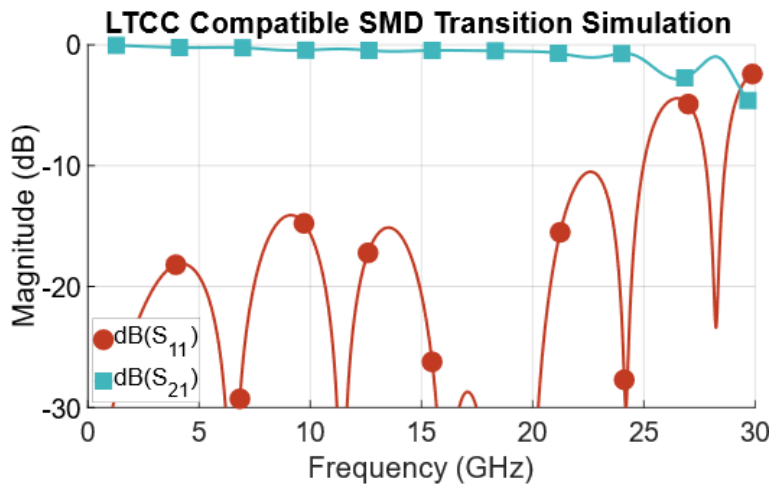


Fig. 4. SMD transition using a metallized half-via

### Y-junction design

The type of circulator designed is a Y-junction circulator with a circular resonator. Impedance matching is achieved using a quarter-wave matching lines. The initial diameter of the resonator is predicted using Bosma's theory [7]. The value of the internal magnetic field in the ferrite, initially assumed to be uniform, is equal to the value obtained by the magnetostatic simulation at the center of the ferrite cylinder. Lastly, the dimensions are optimized while considering the non-uniformity of the static field inside the ferrite by coupling a magnetostatic simulation to the electromagnetic one.

### SMD circulator simulations

The simulated structure is shown in Fig. 1. Minimal adjustments to the impedance matching of the resonator were required after combining the SMD transitions and the circulator design. The circulators have external dimensions of 7×7mm<sup>2</sup>. The simulation reference planes are brought down to the level of the SMD transitions using de-embedding.

The simulated S-parameters of the optimized Garnet SMD LTCC circulator are shown in Fig. 5. The minimum insertion loss is 0.51dB at 16.22GHz. The bandwidth at -18dB is 2.16GHz (BW%>13%, centred around 16.61GHz) with maximum insertion losses of 0.72dB over this bandwidth.

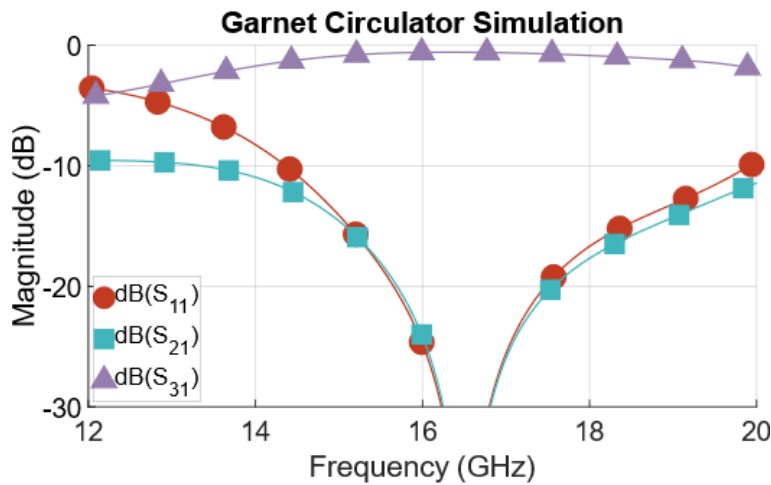


Fig. 5. Garnet SMD circulator simulation

The simulated S-parameters of the optimized Spinel SMD LTCC circulator are shown in Fig. 6. The minimum insertion loss is 0.47dB at 16.29GHz. The bandwidth at -18dB is 3.16GHz (BW%>18.7%, centered around 16.85GHz) with maximum insertion losses of 0.64dB over the band.

The -18dB bandwidth of the spinel circulator is 1GHz wider than that of the garnet circulator. This difference increases even more if the focus is on the -15dB bandwidth. This increase in bandwidth is explained by the higher saturation magnetization of the spinel ferrite (3800G) compared to the garnet ferrite (1900G).

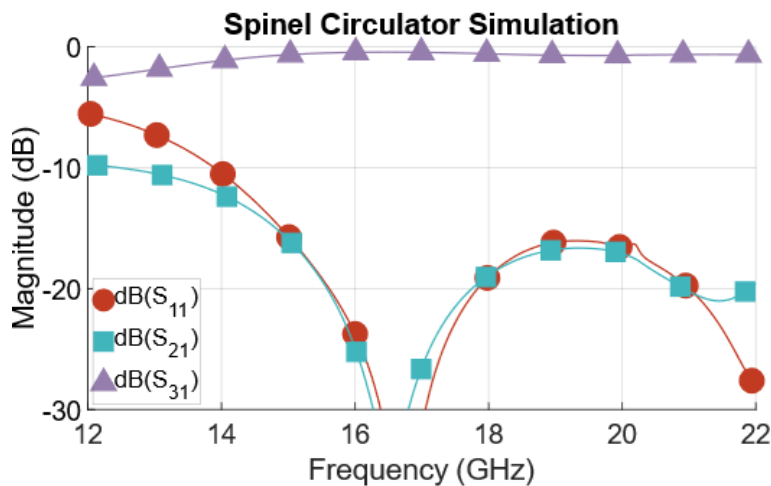


Fig. 6. Spinel SMD circulator simulation

## SMD CIRCULATOR DESIGN

To improve and simplify the manufacture of circulators, a device construction method based on stacking and sintering layers of material, known as LTCC (Low Temperature Cofired Ceramics), has been used. This method makes it possible to integrate more functionality into the device, such as tracks within the structure or vias with solder pads to create an SMD component. Another advantage of this technology is the wide variety of devices that can be produced simultaneously.

The objective is to obtain circulators with dimensions of 7mm×7mm×0.352mm. The maximum surface area available for manufacturing LTCC substrates is 34×34mm<sup>2</sup> with the equipment used. This large area allows the fabrication of up to sixteen circulators in a single run.

The operations involved in the manufacture of the circulators are detailed below:

1. Laser cutting of alignment holes, cavities and inserts
2. Filling the vias with metallic ink
3. Stacking of layers and insertion of ferrite inserts
4. Lamination
5. Screen printing of ground plane and Y-junction with metallic ink
6. Cutting
7. Sintering

Fig. 7 and Fig. 8 illustrate two of the circulator manufacturing stages listed above.

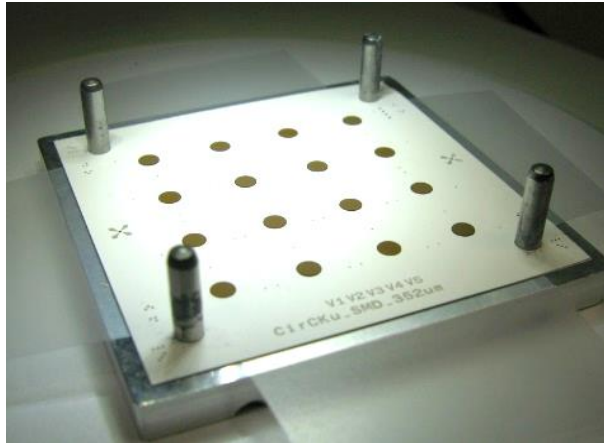


Fig. 7. Stacking of the dielectric layers and the ferrite inserts

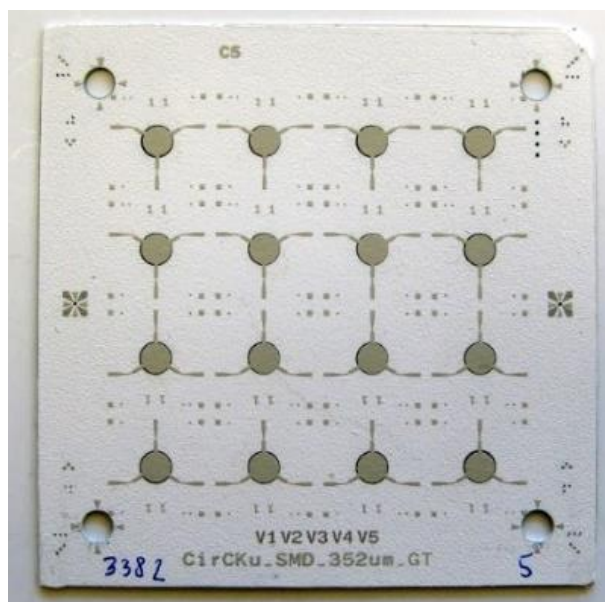


Fig. 8. Screen printing of the Y-junction after the lamination step

The low thickness of the component that allows ensuring good electromagnetic performance, could induce deformation problems during sintering. To avoid this issue, an alumina plate is placed on top of the layer assembly during firing. Two sheets of Separation Powder Sheet (or SPS) are interposed between the two outer faces of the assembly and the alumina plates to prevent the metallization from sticking to the firing plates.

### SMD COMPONENT SOLDERING

To stiffen the test circuit for ease of handling and the tightening of the connectors, the final stack is completed with additional layers of Rogers 4003 to reach a total thickness of approximately 1mm. A symmetrical stack order is used, following a manufacturing recommendation. The aim is to avoid deformation of the transfer substrate during the assembly process. The finish is ENIG (Ni7 $\mu$ m/Au<0.1 $\mu$ m). This finish facilitates component soldering by optimizing the intermetallic interface. The downside is significant line loss.

A view of a soldered circulator is pictured in Fig. 9. An X-ray visual inspection, shown in Fig. 10, was performed to validate the soldering process with a very satisfactory ratio of missing solder to ground plane surface area.

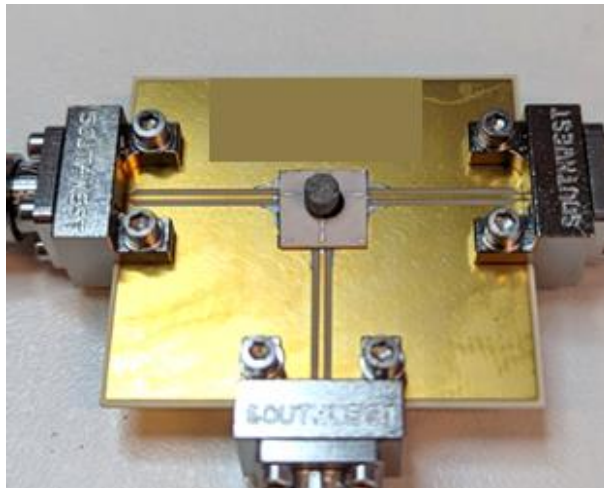


Fig. 9. Soldered circulator

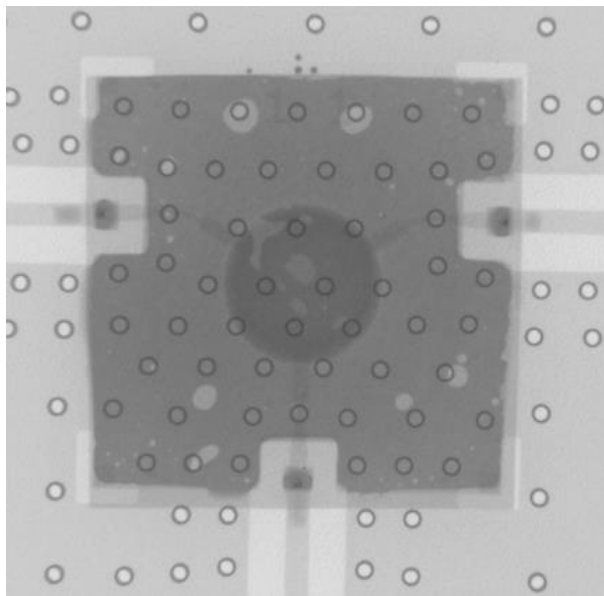


Fig. 10. X-ray observation of the soldered circulator

## MEASUREMENTS

The network analyzer used for the measurements is a Rohde & Schwartz ZVA-67, which allows measurements on three ports. The circulators are connected using Southwest Microwave connectors, reference 292-07A-6. Calibration was performed using a tailor-made TRL calibration kit.

Fig. 11 shows the performance of the soldered Garnet circulator. The device has minimum insertion losses of 0.48dB at 14.48GHz. The bandwidth at -18dB is close to the simulated value at 2.38GHz (BW%>15.6%, centered around 15.17GHz) with maximum insertion losses of 0.8dB. A frequency shift towards the low frequencies of the order of 1.5GHz is observed.

Fig. 12 shows the performance of the soldered Spinel circulator. The device has minimum insertion losses of 0.47dB at 15.88GHz. The bandwidth at -18dB is wider than expected at 5.68GHz (BW%>32%, centered around 17.7GHz) with maximum insertion losses of 0.73dB.

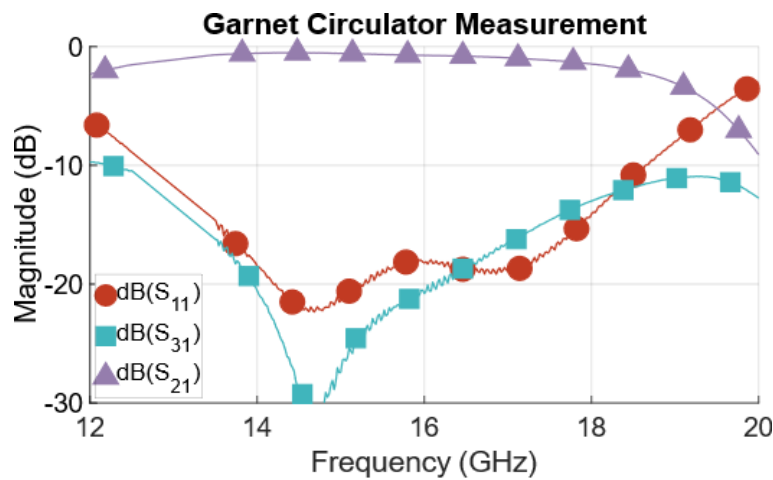


Fig. 11. Measured performances of the soldered Garnet circulator

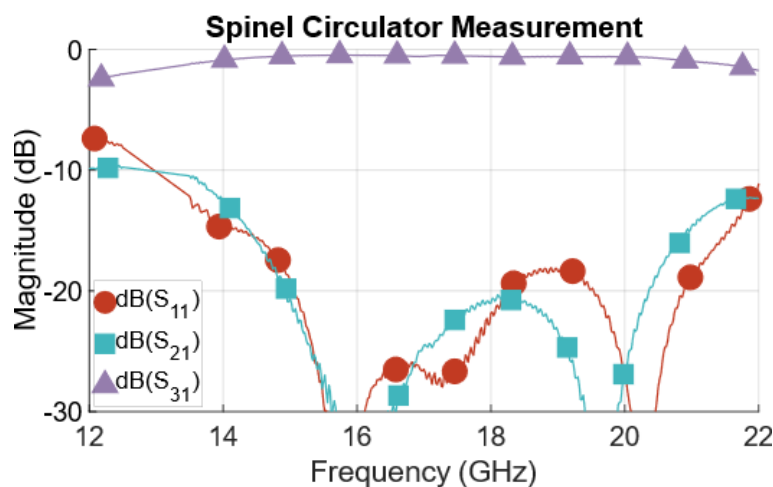


Fig. 12. Measured performances of the soldered Spinel circulator

## CONCLUSION

For the first time to the authors knowledge, low-loss circulators using LTCC technology compatible with SMD technology have been produced. Furthermore, they were successfully soldered to a printed circuit board using the conventional SMD transfer process and were measured.

The successful soldering of the circulators on the transfer board was observed via an X-ray observation. The correct operation of both the LTCC compatible SMD transition as well as the circulator designs were verified through the measurement of electromagnetic performance close to those expected.

The two circulators presented here are currently state of the art in terms of insertion loss in Ku band for LTCC circulators, despite the addition of SMD transitions. Both the measured bandwidths at -18dB exceeded the expectations with an increase of almost 80% for the spinel circulator.

## ACKNOWLEDGMENT

The authors would like to thank the Agence Innovation Défense and the Agence Nationale de la Recherche for the financial support they provided for this work.

## REFERENCES

- [1] T. Jensen, V. Krozer, and C. Kjærgaard, "Realisation of microstrip junction circulator using LTCC technology," *Electron. Lett.*, vol. 47, no. 2, p. 111, 2011, doi: 10.1049/el.2010.2419.
- [2] R. van Dijk, G. van der Bent, M. Ashari, and M. McKay, "Circulator integrated in low temperature co-fired ceramics technology," in *2014 44th European Microwave Conference*, Rome: IEEE, Oct. 2014, pp. 1544–1547. doi: 10.1109/EuMC.2014.6986744.

- [3] P. R. Raj, A. Basu, and S. K. Koul, "Comparison of triangular geometries of Y-junction in co-sintered LTCC based microstrip circulator," in 2017 IEEE MTT-S International Microwave Workshop Series on Advanced Materials and Processes for RF and THz Applications (IMWS-AMP), Pavia: IEEE, Sep. 2017, pp. 1–3. doi: 10.1109/IMWS-AMP.2017.8247361.
- [4] L. Qassym, V. Laur, R. Lebourgeois, and P. Queffelec, "Ferrimagnetic garnets for Low Temperature Co-fired Ceramics microwave circulators," in 2018 IEEE/MTT-S International Microwave Symposium - IMS, Philadelphia, PA: IEEE, Jun. 2018, pp. 750–752. doi: 10.1109/MWSYM.2018.8439250.
- [5] S. Yang, W. Shi, H. Bai, and T. Zhang, "Circulator Integrated in LTCC with Screen Printed Co-Firing Ferrite for Space Application," in 2018 International Conference on Microwave and Millimeter Wave Technology (ICMMT), Chengdu: IEEE, May 2018, pp. 1–3. doi: 10.1109/ICMMT.2018.8563702.
- [6] N. Parker et al., "Ku-Band Microstrip Junction Circulators Manufactured using Low Temperature Co-fired Ceramics Technology," in 2022 Asia-Pacific Microwave Conference (APMC), Yokohama, Japan: IEEE, Nov. 2022, pp. 112–114. doi: 10.23919/APMC55665.2022.10000006.
- [7] H. Bosma, "On Stripline Y-Circulation at UHF," IEEE Trans. Microw. Theory Tech., vol. 12, no. 1, pp. 61–72, Jan. 1964, doi: 10.1109/TMTT.1964.1125753.